Electrocatalytic activity of sodium tetrafluorocuprate modified gold electrode for glucose determination

Hong-Wei Lv, Quan-Fu Li, Hui-Ling Peng[*]

College of Electronic Engineering, Guangxi Normal University. Guilin541004. China
[*]E-mail: penghuiling1008@163.com

Sodium tetrafluorocuprate (Na_2CuF_4) has been synthesized by the precipitation method. Then, Na_2CuF_4 was applied to glucose electrocatalysis for the first time, and modified bare Au electrode to obtain Na_2CuF_4/Au. Na_2CuF_4/Au has strong anti-interference, extremely broad linear range of glucose detection, and great stability through stored for a long time at room temperature. A simple method was used to prepare Na_2CuF_4 with different morphologies, and the effects of different morphologies for the glucose sensing performance were studied. The optimal experimental parameters of glucose sensing were obtained through parameter optimization, which leads to enhanced glucose sensing performance. The selected Na_2CuF_4 was composed of large crystals and smaller crystals. The larger crystals sizes of selected Na_2CuF_4 are in the range from 5 μm to 6 μm, and the smaller are in the range from 230 nm to 300 nm, the two are mixed together. The Na_2CuF_4/Au electrode showed high sensitivity and very wide linear range (the first 0.01-0.15 mM, the second 0.15-19.15 mM, the third 19.15-63.15 mM). The Na_2CuF_4/Au shows good accuracy, reproducibility and stability, as well as excellent selectivity. The properties of Na_2CuF_4 indicate that it has a wide application prospect in the field of glucose electrocatalysis as a new glucose sensitive material.

Keywords: Sodium tetrafluorocuprate; Non-enzymatic sensor; Glucose detection; Wide linear range; Modified Au electrode

1. INTRODUCTION

Diabetes mellitus, caused by the inadequate production of insulin by the pancreas or the inability to utilize insulin effectively, leads to higher plasma glucose content than the normal level ultimately [1,2]. Its incidence have steadily increased in the recent decades and turns to be one of the most serious public health problems in the global world [3,4]. The best way of avoiding possible diabetic emergency is monitor the blood glucose level, such as, fast and sensitive blood glucose monitoring devices are commonly used as medical devices in the management of diabetes. Electrochemical method of

determining glucose is playing an important role in many fields due to its simple fabrication process, excellent stability, and electro-chemical performance [5]. The electrochemical method contains enzyme-based glucose and non-enzymatic glucose sensing. Glucose oxidase (GOx) and glucose dehydrogenase (GDH) are the most commonly used enzymes in enzyme-based glucose sensors [6,7]. The application of enzyme sensor is limited by its high cost, complicated immobilization process of enzymes, and inherent instability [8,9]. Non-enzymatic glucose sensor based on electrochemical reaction has recently attracted more attention due to its advantages including simplicity, reproducibility and inexpensive [1]. More importantly, non-enzyme sensors are not restricted by oxygen, oxygen concentrations may modulate the sensor signal of enzyme-based glucose sensor [10-13]. Hence, much interest has been focused on developing electrochemical non-enzymatic glucose sensor. Different nanomaterials such as metal materials CuO [14], Au [15], Pt [16], Mn_3O_4 [17], boronic acid (BA) [18] and alloys (Au-Cu [19], Au-Pt [20]) have been explored as electrode material to fabricate the non-enzymatic sensors for the glucose determination. However, the recently reported materials have been difficult in practical applications for glucose sensing because of the complexity of preparations [19], the high cost [20], and the narrow linear range of glucose detection [17]. Therefore, we studied the synthesis of metal-based materials, especially the transition metal copper.

Herein, Na_2CuF_4 was synthesized by a precipitation method. The modified electrode has excellent glucose sensing performance especially extremely broad linear range of glucose detection. This is the first report of Na_2CuF_4 as sensitive material for glucose detection and modified electrode to be incorporated into a non-enzymatic glucose sensor system. The experimental parameters were optimized to obtain the highest-sensitivity of the electrode. The electrode was evaluated for its glucose sensing performance, the anti-interference performance of Na_2CuF_4 modified electrode was tested in artificial sweat, which confirmed potential applications of Na_2CuF_4 to glucose detection in human body fluids.

2. EXPERIMENT

2.1. Reagents and chemicals

Cupric chloride dihydrate ($CuCl_2 \cdot 2H_2O$), hydrofluoric acid (HF), sodium hydroxide (NaOH), sulfuric acid (H_2SO_4), glucose, sodium chloride (NaCl), ammonium chloride (NH_4Cl), acetic acid, DL-lactic acid, uric acid (UA), dopamine hydrochloride (DA), ascorbic acid (AA), D-(+)-galactose, lactose, sucrose, etc. were all supplied by Shanghai Aladdin technology limited liability company. All the other chemicals used in this work were analyzable grade and were used without further purification. All solutions were prepared in deionized water.

2.2. Equipments

Scanning electron microscopy (SEM) images were taken by a JSM-IT300 (JEOL, Ltd., Japan). Electrochemical tests adopted CS2350 electrochemical workstation (Corrtest Instruments Corp., Ltd.,

Wuhan, China). XRD pattern was determined by an XRD (XD-6) at ambient temperature. ICP analysis adopted Flexar/NexlON300X HPLC-ICP-MS (PerKinEler).

2.3. The preparation of Na_2CuF_4

Na_2CuF_4 nanoparticles were prepared by a precipitation method. By change the mass of $CuCl_2·2H_2O$ in the reactant to control the composition of the precursor, six kinds of Na_2CuF_4 with different morphologies were prepared in this work. First of all, six $CuCl_2·2H_2O$ with different mass (0.1 g, 0.5 g, 2 g, 4 g, 6 g, 8 g) were mixed with 10 ml 40% HF, separately. For all the mixed solution, deionized water was added and the final volume was fixed at 20 ml to obtain the precursor solution. Then, slowly drip NaOH solution into the precursor with stirring continuously [36], the white precipitate Na_2CuF_4 was gradually formed. After that, the white precipitate was collected by centrifugation and washed with deionized water several times to remove the excess reactants and other soluble substances in deionized water. After drying at 60°C, the white Na_2CuF_4 powder was obtained and stored in dry environment at room temperature.

2.4. Preparation of modified electrode

Firstly, 10 mg of the prepared Na_2CuF_4 powder was added to 10 ml deionized water and sonicated for 20 min to obtain the Na_2CuF_4 suspension (1 $mg·ml^{-1}$). Before modification, the bare Au electrode was polished, washed several times under ultrasound with deionized water and anhydrous ethanol, then dried in nitrogen stream. Then 20 μL Na_2CuF_4 suspension was transferred onto the bare Au electrode, then dried in air and repeat 5 times. After drying, a small amount of Nafion (0.5 wt %) was dripped onto the modified Au electrode, and then dried in air again to obtain Na_2CuF_4/Au. The fabricated electrodes were stored in a dry environment at room temperature for further use. Nafion is commonly used as an electrode modifier [22] for fixation of electrode materials, with a good selective permeability [23], the selectivity and stability to glucose detection of the electrode can be improved.

2.5. The fabrication of artificial sweat

The artificial sweat was prepared according to the standard ISO 3160-2, containing 20 $g·L^{-1}$ NaCl, 17.5 $g·L^{-1}$ NH_4Cl, 5 $g·L^{-1}$ acetic acid and 15 $g·L^{-1}$ lactic acid. The pH of the artificial sweat was adjusted to 13 and 0.66 M NaOH was added. Glucose was added into artificial sweat to obtain samples with different glucose concentrations. The test was performed by electrochemical workstation with amperometric mode at a voltage of 0.1 V [21].

2.6. Electrochemical measurement

The traditional three-electrode system, including bare gold working electrode, Na_2CuF_4 modified gold-based working electrode, saturated calomel electrode (SCE) reference electrode and platinum wire

counter electrode, were used for electrochemical measurement in the CS series Electrochemical Workstation. Under continuous agitation, current-time curve (I-t) were recorded at a certain applied potential.

3. RESULTS AND DISCUSSION

3.1. Preparation and characterization of Na_2CuF_4

The above scheme describes the preparation process of Na_2CuF_4. Firstly, $CuCl_2 \cdot 2H_2O$ was dissolved in HF, and then NaOH solution was added. By adjusting the pH of the solution to near-neutral, Na_2CuF_4 was precipitated. During the preparation of materials, effective heat dissipation of the reaction system should be ensured, and the drop of NaOH needs to be slow to prevent overheating and the formation of the blue copper hydroxide precipitate, which then decomposed into the black copper oxide precipitate. According to other work [36], CuF_4^{2-} was prepared by more complex methods. Based on this, we simplified the experimental steps and obtained stable Na_2CuF_4 use a simpler method. This preparation method is simple to operate and the phenomenon is easy to observe, the generation of Na_2CuF_4 can be effectively determined through the appearance of white precipitation. In addition, Na_2CuF_4 with different morphologies were generated according to different Cu^{2+} content in the precursor solution. These different Na_2CuF_4 have distinct glucose oxidation activities.
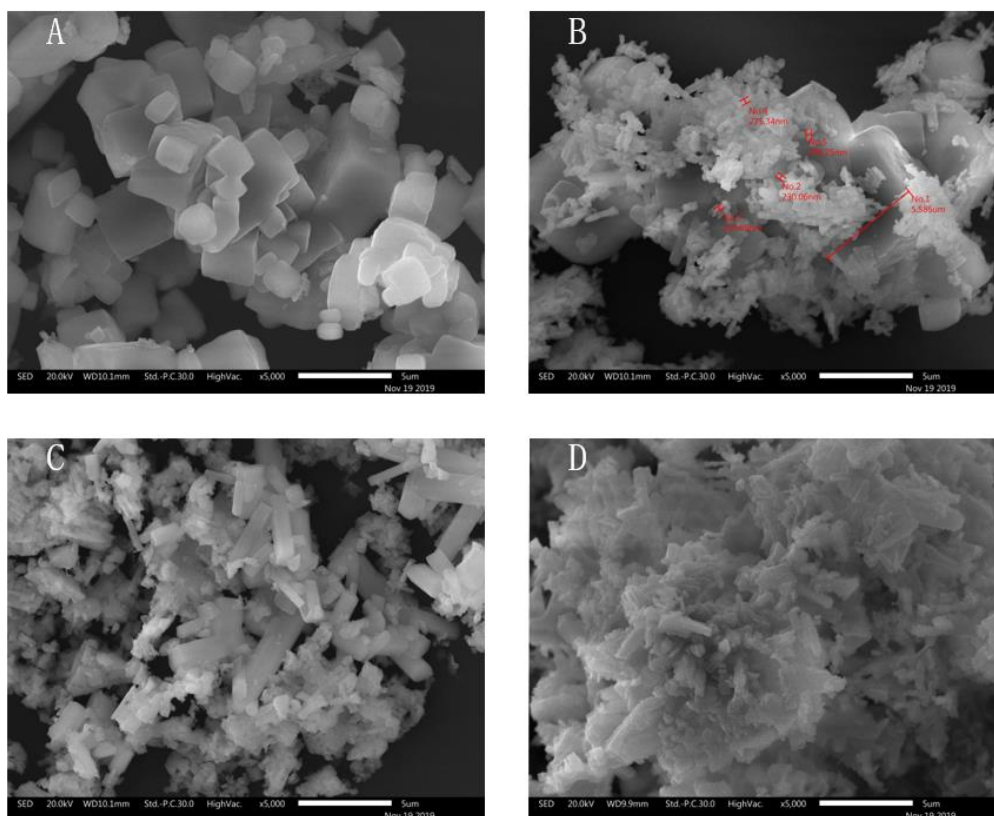

Figure 1. SEM images of Na_2CuF_4 with different mass of reactant of (A) 0.1 g $CuCl_2 \cdot 2H_2O$, (B) 2 g $CuCl_2 \cdot 2H_2O$, (C) 4 g $CuCl_2 \cdot 2H_2O$, (D) 8 g $CuCl_2 \cdot 2H_2O$.

The morphologies of Na_2CuF_4 powder were examined by SEM. The morphology of Na_2CuF_4 was controlled by change the mass of the reactant, precisely, $CuCl_2 \cdot 2H_2O$. As shown in Fig.1, the morphology of Na_2CuF_4 changed with the increase of the mass of $CuCl_2 \cdot 2H_2O$. When the reactant concentration is low, Na_2CuF_4 crystals with 0.1 g $CuCl_2 \cdot 2H_2O$ mainly exists in the form of flakes and blocks, with a size between 2 μm and 3 μm, and a small number of smaller crystals exist, as shown in Fig.1A. As the increases of the reactant concentration, the size of crystal increase, meanwhile, the number of smaller crystals also increased. As shown in Fig.1B, Na_2CuF_4 crystals with 2 g $CuCl_2 \cdot 2H_2O$, the size of large crystals between 5 μm and 6 μm, smaller crystals between 230 nm and 300 nm, the two are mixed together in direct contact. As the mass of $CuCl_2 \cdot 2H_2O$ increased to 4 g, the large flake and block crystals transformed into four-square columnar crystals of 3 to 5 μm in length, while the smaller crystals increase continuously, as shown in Fig.1C. As the mass of $CuCl_2 \cdot 2H_2O$ increased to 8 g, the smaller crystals increase continuously, and the large crystals are almost surrounded by smaller crystals, as shown in Fig.1D. It can be predicted that the Na_2CuF_4 materials prepared by the above scheme would supply rich active sites and significantly promote mass and electron transfer for glucose sensing. Its inherent high catalytic activity of glucose will make the Na_2CuF_4 prepared by this method an excellent electrocatalyst.
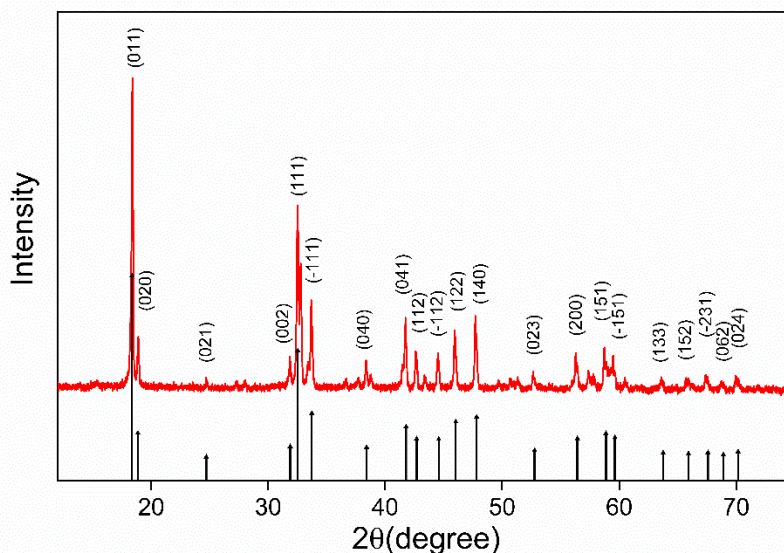

Figure 2. XRD pattern of the synthesized Na_2CuF_4 materials.

The Na_2CuF_4 powder was studied by XRD, as shown in Fig.2. The strong diffraction peaks at 18.5°, 19.0°, 24.8°, 32.0°, 32.6°, 33.8°, 38.5°, 41.8°, 42.8°, 44.6°, 46.1°, 47.9°, 52.8°, 56.5°, 58.9°, 59.7°, 63.8°, 65.9°, 67.6°, 68.9° and 70.2° could be assigned to the (011), (020), (021), (002), (111), (-111), (040), (041), (112), (-112), (122), (140), (023), (200), (151), (-151), (133), (152), (-231), (062) and (024) planes of Na_2CuF_4. All these peaks are consistent with the data of JCPDS Na_2CuF_4 (76-0732) in the range 20-80°. It indicated that Na_2CuF_4 was prepared by the precipitation method successfully. The sample was highly crystalline in nature can be proved by the peak intensities and widths. The results showed that the final sample was all with the purity of the Na_2CuF_4 phase.

The elemental composition of Na_2CuF_4 was obtained by HPLC-ICP-MS at 60 μg·L^{-1}. As a result,

6mg samples of Na_2CuF_4 contains 1.7 mg Na and 2.2 mg Cu, which in conformity with the mass ratio of Na/Cu in Na_2CuF_4 (46/64). This result is consistent with the XRD analyses.

3.2. Electrochemical characteristics of Na_2CuF_4

        Firstly, the electrochemical behavior of six kinds of Na_2CuF_4 materials with different morphologies was studied by cyclic voltammetry (CV) in the presence of 1mM glucose under alkaline conditions. As shown in Fig.3A, the Na_2CuF_4 materials prepared by 2 g $CuCl_2 \cdot 2H_2O$ have the best glucose sensing performance because of the wide anode peak around 0 V and the value of current subsequently, as well as the cathode peak at -0.35 V. Fig.3B shows the value of peak-anode current at 0 V of six kinds of Na_2CuF_4 with different morphologies in Fig.3A. As the mass of $CuCl_2 \cdot 2H_2O$ increased from 0.1 g to 2 g, the value of peak current increased, which is synchronized with the increase of smaller crystals shown in Fig.1. In addition, the mass of $CuCl_2 \cdot 2H_2O$ increased from 4 g to 8 g, corresponding to Fig.1, the number of smaller crystals increased, and the peak current also increased. It can be seen that the increase of smaller crystals lead to the increase of the value of peak-anode current. When the mass of $CuCl_2 \cdot 2H_2O$ increased from 2 g to 4 g, the value of peak-anode current decreased significantly in Fig.3B. Meanwhile, according to the results in Fig.1, the large flake and block crystals transformed into four-square columnar crystals of 3 to 5 μm in length. From this it can be inferred that the morphological changes are responsible for the decrease of the value of peak-anode current. In summary, as shown in Fig.3B, the morphology of Na_2CuF_4 changed with the mass of $CuCl_2 \cdot 2H_2O$, and the mass of $CuCl_2 \cdot 2H_2O$ increased from 0.1 g to 2 g, the number of smaller crystals also increased. These smaller crystals make Na_2CuF_4 have larger surface area and more active sites, its glucose sensing performance also increased. When the mass of $CuCl_2 \cdot 2H_2O$ increased to 4 g, the morphology of Na_2CuF_4 further changed, and the shape of the larger crystals changed from flake and block to four-square columnar, which reduced the performance of glucose sensing significantly. After that, the number of smaller crystals increased with the mass of $CuCl_2 \cdot 2H_2O$, while the glucose sensing performance increased synchronously. According to the results in Fig.3, Na_2CuF_4 materials with the mass of $CuCl_2 \cdot 2H_2O$ of 2 g have the best glucose sensing performance, and it was selected for further testing.
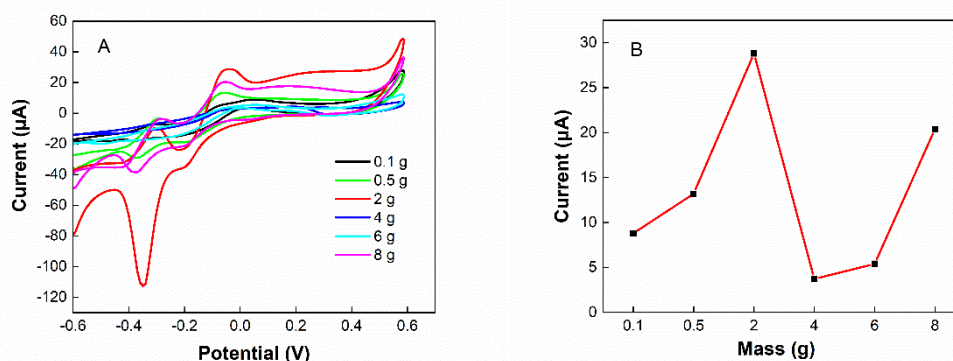

Figure 3. (A) CV curves of Na_2CuF_4/Au with different mass of $CuCl_2 \cdot 2H_2O$. Scan rate: 20 mV·s⁻¹. (B) The value of peak-anode current of different Na_2CuF_4 materials in 3A.

Figure 4. (A) CV curves of Na_2CuF_4/Au and bare Au in 0.5 M H_2SO_4 solution. Scan rate: 20 mV·s^{-1}. (B) CV curves of bare Au in 0.1 M NaOH in the absence and presence of 1 mM, 2 mM glucose. Scan rate: 20 mV·s^{-1}. (C) CV curves of Na_2CuF_4/Au in 0.1 M NaOH in the absence and presence of 1 mM, 2 mM glucose. Scan rate: 20 mV·s^{-1}. (D) CV curves of bare Au and Na_2CuF_4/Au in 0.1 M NaOH with 1 mM glucose. Scan rate: 20 mV·s^{-1}.

In order to test the electrochemical active surface area of Na_2CuF_4/Au electrode, the electrochemical behaviors of bare Au and Na_2CuF_4/Au electrode in 0.5 M H_2SO_4 solution were studied by cyclic voltammetry (CV). As shown in Fig.4A, both of the blue line and red line, broad anode peaks are observed at 1.1 V, which correspond to the formation of Au_2O_3 [24]. During the reverse cathodic scan, the reduction peaks are observed due to the reduction of gold oxide at 1.02 V, these are consistent with the electrochemical behavior of Au element [20,24]. As can be seen from the blue line of bare Au electrode in Fig.4A, the direction and potential of the two redox peaks were the same as that of the Na_2CuF_4/Au electrode. The value of peak current of Na_2CuF_4/Au electrode was higher significantly than that of bare Au electrode. It indicated that Na_2CuF_4/Au electrode has larger electrochemically active surface area than that of bare Au electrode. According to other work [39], the larger electrochemically active surface area may provide more active sites for modified Au electrode, which is an important prerequisite for efficient electrocatalysis and glucose sensing. That means Na_2CuF_4/Au has a good electrochemical detection capability.

The electrocatalytic activities of bare Au electrode (4B) and Na_2CuF_4/Au electrode (4C) for glucose oxidation were studied by cyclic voltammetry, the curves were obtained in 0.1 M NaOH solution without glucose, containing 1 mM glucose and 2 mM glucose. In the absence of glucose, the CV curve of Au electrode shows the characteristics including the anodic peak of the oxidation of Au to

Au_2O_3 and the cathode peak of the reduction of Au_2O_3 [24]. After the addition of glucose, the CV curve of bare Au electrode changed greatly, and a series of complex electrochemical reactions occurred simultaneously. During the forward scan, two new oxidation peaks were observed at -0.1 V and +0.3 V, correspond to the formation of gluconolactone and further oxidation of gluconolactone, respectively. With the potential continues to rise, the oxidation of gluconolactone was end due to the formation of Au_2O_3 and the reduction of AuOH active site. In the process of negative scan, Au_2O_3 is reduced and AuOH is generated again to promote the oxidation of glucose, an obvious anode peak appears at +0.2 V. As for the Na_2CuF_4/Au electrode, it can be seen from the different CV curves between Fig.4B and 4C that the reaction principle of electrocatalytic oxidation of glucose on Na_2CuF_4/Au is completely different from that of Au electrode, and Na_2CuF_4/Au is more sensitive to glucose than that of bare Au electrode. Hence, the CV curves completely changed under the same conditions after Au electrode modified by Na_2CuF_4. During the forward scan, as shown in Fig.4D, Na_2CuF_4/Au electrode produced two anode peaks, peak 1 at -0.3 V and peak 2 at 0 V. Peak 1 may be related to the Au electrode itself, at the same time, in the position of the peak 1, Cu(II) began to form complex with glucose and gradually be oxidized to Cu(III)-glucose, in the position of the peak 2, the oxidation steps of Cu(II)-glucose to Cu(III)-glucose go further. Cu(III)-glucose is not stable, in the process of retrace, Cu(III)-glucose is easily reduced to Cu(II) and gluconolactone through the redox reaction [37,38], gluconolactone further hydrolyzed into glucose acid, this series of reactions lead to the formation of the reduction peak during the retrace process, namely peak 3 at -0.2 V and peak 4 at -0.35 V. As shown in Fig.4C, after glucose was added, the oxidation peak current increased but the reduction peak current decreased slightly, indicated that Na_2CuF_4 could electrocatalytic oxidation of glucose in NaOH solution, which was similar to CuO under alkaline conditions [25]. Compared the value of current in Fig.4B and 4C under the same conditions, it can be found that the current of bare Au electrode is lower, indicated that modification of Na_2CuF_4 materials improved the glucose sensing performance of Au electrode significantly.

More intuitively, in order to show the glucose sensing performance of Na_2CuF_4/Au is affected by Na_2CuF_4, as shown in Fig.4D, CV curves of bare Au and Na_2CuF_4/Au electrode in 0.1 M NaOH solution with 1 mM glucose. The oxidation peak and reduction peak of the Na_2CuF_4/Au electrode were more obvious with greater redox peak current of CV. The results showed that the prepared Na_2CuF_4 improved the glucose sensing performance of modified Au electrode significantly.

In order to determine the dependence of electrochemical signals on glucose concentration, the potential was kept at 0.1 V in 0.1 M NaOH solution, and the ampere response of Na_2CuF_4/Au electrode by continuous glucose injection was studied. The current-time curve (I-t) is shown in Fig.5A. The results shown that the current intensity on Na_2CuF_4/Au electrode increases with the accretion of glucose. The calibration curve of Na_2CuF_4/Au electrode is described in Fig.5B, and three linear ranges can be found, with slopes of 344.52 $\mu A \cdot mM^{-1} \cdot cm^{-2}$, 94.20 $\mu A \cdot mM^{-1} \cdot cm^{-2}$ and 353.31 $\mu A \cdot mM^{-1} \cdot cm^{-2}$, respectively.

The sensitivity in the first (0.01-0.15 mM), the second (0.15-19.15 mM) and the third (19.15-63.15 mM) linear range are 229.68 $\mu A \cdot mM^{-1} \cdot cm^{-2}$, 62.8 $\mu A \cdot mM^{-1} \cdot cm^{-2}$ and 235.54 $\mu A \cdot mM^{-1} \cdot cm^{-2}$, respectively, the limit of detection (LOD) was measured by the experiment as 0.5 μM. Na_2CuF_4 prepared by this method has unique morphology, large electrochemically active surface areas and abundant active sites. Meanwhile, through the synergism of Na_2CuF_4 and Au electrode, this non-enzymatic glucose sensor has a high sensitivity.

Table 1. Performance comparison between Na_2CuF_4/Au and other reported glucose sensors.

Electrode matrix	Linear range(mM)	Sensitivity ($\mu A \cdot mM^{-1} \cdot cm^{-2}$)	Detection limit(μM)	Ref.
Cu@Cu$_2$O NPs/GCE	0.01-5.5	123.8	0.05	[27]
Cu$_2$O Nanothorn array/Cu foam	N/A	97.9	0.005	[28]
CuO Nano leaf/ ZnO NR/Cu sheet	0.1-1	408	18	[29]
Cu@Cu$_2$O NS/ rGO/GCE	0.005-7	145.2	0.5	[30]
CuO NP/N-G/ GCE	0.001-6	207.3	0.5	[31]
CuO NWs/GCE	0.0005-0.488, 0.988-5.488	64.1, 488	0.045	[32]
Cu$_2$O Porous NS/ rGO/GCE	0.01-6	185	0.05	[33]
Cu$_2$O Hollow NC/GCE	0.001-1.7	52.5	0.87	[34]
Cu NPs N-doped carbon/GCE	0.005-2.1, 2.6-10	223.6, 100.6	5	[35]
Na$_2$CuF$_4$/Au	0.01-0.15, 0.15-19.15, 19.15-63.15	229.68, 62.8, 235.54	0.5	This work

NPs: nanoparticles. GCE: glassy carbon electrode. NR: nanorod. NS: nanostructured. NWs: nanowires. rGO: reduced graphene oxide. NC: nanocubes.

The performances of glucose detection of the fabricated electrode and the reported Cu or CuO based electrodes are shown in Table 1 [27–35]. The LOD and sensitivity of the prepared Na_2CuF_4/Au electrode is in the normal range of other reported sensors. However, the linear range of Na_2CuF_4/Au is extremely broad from 0.01 mM to 63.15 mM. In the case of CuO Nano leaf/Cu sheet [29], the sensitivity is higher, but the LOD was much higher and linear range was much smaller (0.1 mM to 1 mM) than that of the Na_2CuF_4/Au electrode. Even for Cu_2O Nanothorn array/Cu foam [28], its linear range was not wide. In fact, the wide linear response is of great significance to practical applications, because it can be adapted to the testing requirements in more occasions [41]. In this work, Na_2CuF_4/Au electrode shows
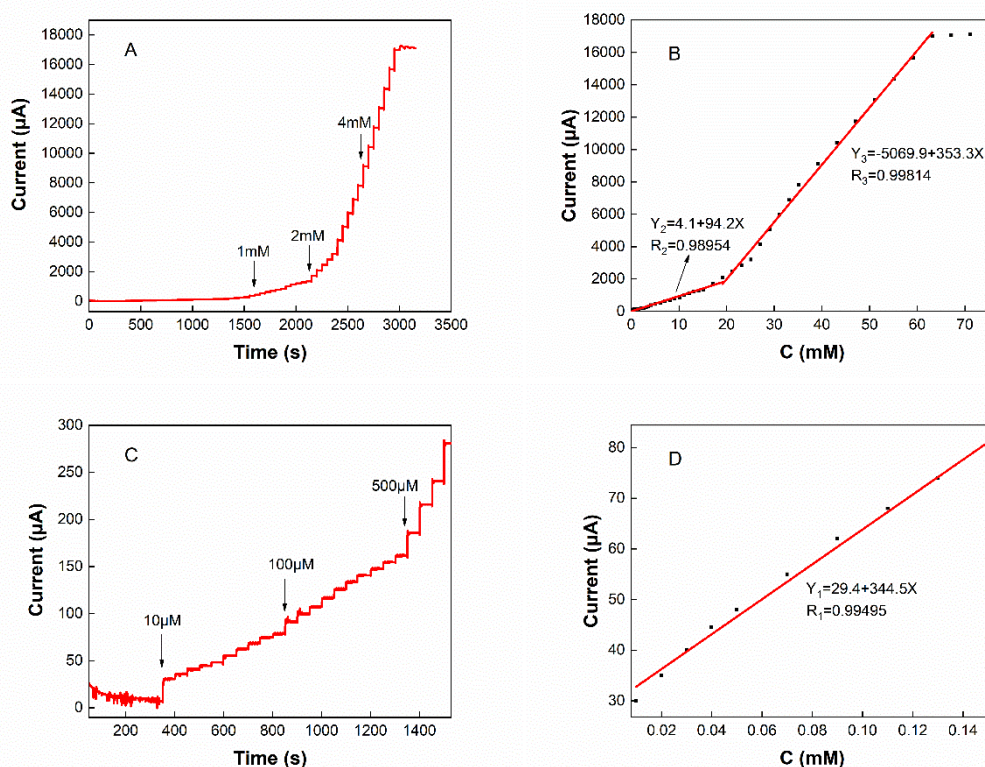
great electrochemical performance in glucose sensing.

Figure 5. (A) Typical I-t curve obtained at Na$_2$CuF$_4$/Au on the successive injection of glucose in 0.1 M NaOH solution with an applied potential of +0.1 V. (B) The typical calibration graph for glucose. (C) Enlarge image of (A). (D) Enlarge image of (B).

3.3. Selectivity, stability and reproducibility of Na$_2$CuF$_4$/Au electrode

The glucose sensor must be able to resist the interference of various interfering substances in human serum or sweat. In general, glucose levels are much higher (at least 10 times higher) than the level of interfering substances in human blood. Hence, the molar ratio used in this work is 10:1 (glucose to each interfering substance). We analyzed the selectivity of Na$_2$CuF$_4$/Au electrode for ascorbic acid (AA), uric acid (UA), dopamine (DA), galactose, lactose, sucrose and other small molecules commonly found in human serum. The results are shown in Fig.6A, the response of the modified electrode to various interfering substances is much less than that of glucose. These results indicated that Na$_2$CuF$_4$ modified Au electrode has a good selectivity.

Under normal circumstances, the lactic acid content in human blood about 1-7 mM, which does not interfere with the glucose detection, according to different exercise conditions. However, the lactic acid in sweat is about 5-60 mM, which is much higher than glucose in sweat [26]. The resistance to lactic acid of electrode materials is necessary for glucose detection in sweat. As shown in Fig.6B, the interference of lactic acid of Na$_2$CuF$_4$/Au electrode was studied. The electrode had no current response roughly after the addition of 5 mM lactic acid, and a low current response appeared after the lactic acid increased to 10 mM. When the lactic acid increased to 50 mM, the response of the electrode to lactic

acid still did not exceed the current response of 1 mM glucose. It indicated that the Na_2CuF_4/Au electrode had great potential in the detection of glucose in sweat.

As for a stability study, the current response kept at the maximum value for a long time (1600 s), as shown in Fig.6C. After 19 days of storage in air tight container at room temperature, the current response only decreased by 2.2%, as shown in Fig.6D. In order to study the influence of environmental variables such as humidity, the electrode was exposed to air for 3 days and tested under similar conditions. It was observed that the current response remained around 95%. In conclusion, the prepared Na_2CuF_4 materials were stable enough to satisfy the needs of the stability requirements of the electrode for the glucose sensor.

To evaluate its reproducibility, 5 electrodes were prepared by the same method. The relative standard deviations (RSDs) for calculating the glucose response of these electrodes were no more than 9.6%. These results indicated that the Na_2CuF_4/Au electrode has good glucose sensing performance.
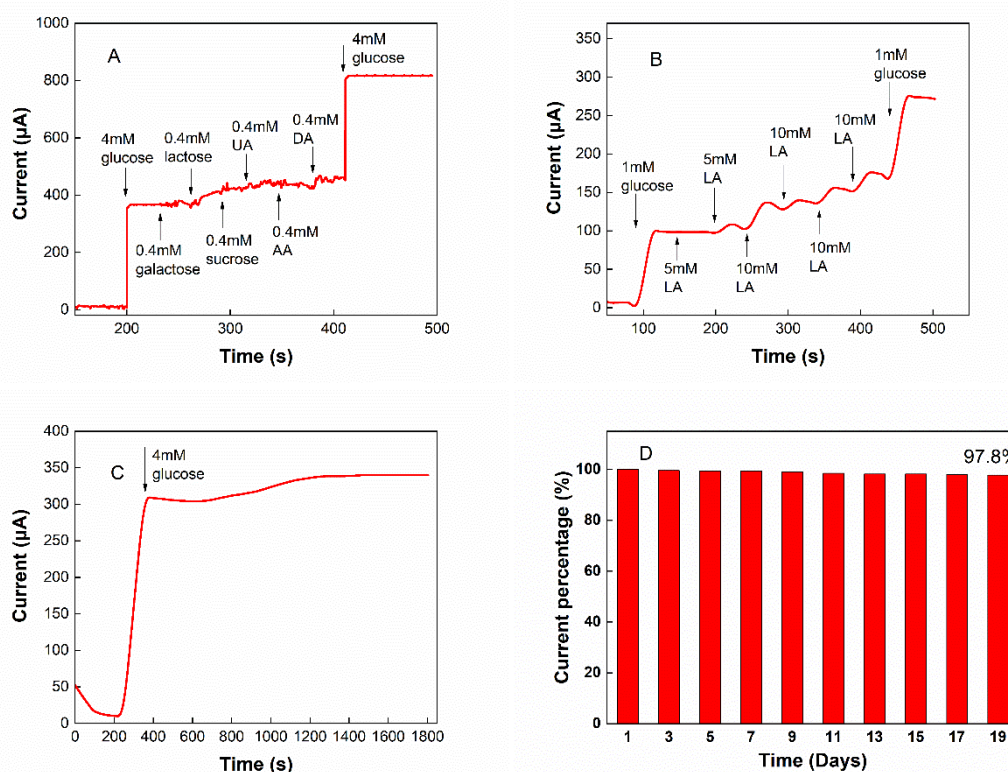

Figure 6. (A) The amperometric response of Na_2CuF_4/Au to successive injections of 4 mM glucose and AA (0.4 mM), UA (0.4 mM), DA (0.4 mM), lactosum (0.4 mM), galactose (0.4 mM), sucrose (0.4 mM). (B) The amperometric response of Na_2CuF_4/Au to successive injections of 1 mM glucose and lactic acid. (C) The amperometric response of Na_2CuF_4/Au for 4 mM glucose during long time (1600 s). (D) Stability of Na_2CuF_4/Au stored in air tight container for 19 days.

3.4. Sweat sample analysis of the Na_2CuF_4/Au

In practical application, glucose in sweat is more difficult to detect than that in blood due to low concentration of glucose and high interference of lactic acid [40]. The practical applicability of the Na_2CuF_4/Au electrode was evaluated by detecting glucose in artificial human sweat. As shown in Table 2, glucose was added to sweat samples with and without glucose continuously, and the detection recovery

was 95-97%, Na_2CuF_4/Au electrode was able to work effectively under conditions with different initial glucose levels. This indicated that Na_2CuF_4/Au electrode was feasible for glucose detection in actual samples of human body fluids.

Table 2. Detection of glucose in artificial sweats.

Sample	Original(μM)	Added(μM)	Found(μM)	Recovery(%)
Sample 1	0	200	194	97.0
	0	1000	965	96.5
Sample 2	200	800	950	95.0

4. CONCLUSION

In summary, Na_2CuF_4 powder was synthesized by a facile and effective method for glucose sensing. The glucose sensing performance of Na_2CuF_4 with different morphologies was investigated. The Na_2CuF_4 with high electrocatalytic activity to glucose was selected through material optimization, and the modified Au electrode was prepared by this material. The fabricated Na_2CuF_4/Au electrode has high sensitivity, extremely wide linear range, good selectivity, stability and reproducibility. Moreover, the electrode has high anti-interference ability to lactic acid, which indicated that the electrode can detect glucose in body fluid. These excellent performances of glucose detection of the Na_2CuF_4/Au electrode and good stability of Na_2CuF_4 materials demonstrate Na_2CuF_4 is an excellent material for the preparation of high-quality non-enzymatic glucose sensors. The application of Na_2CuF_4 to electrochemical detection of glucose in this work opens up new ideas for commercial glucose sensor and sets a typical example for the production of high-quality nanomaterials for sensing applications.

References

1. D.W. Hwang, S. Lee, M. Seo, T.D. Chung, *Anal. Chim. Acta*, 1033 (2018) 1–34.
2. Y. Hu, X. Niu, H. Zhao, J. Tang, M. Lan, *Electrochim. Acta*, 165 (2015) 383–389.
3. K.G.M.M. Alberti, P.Z. Zimmet, *Diabet. Med.*, 15 (1998) 539–553.
4. M. Heller, P. Edelstein, M. Mayer, *BBA - Biomembr.*, 413 (1975) 472–482.
5. Z. Pu, R. Wang, J. Wu, H. Yu, K. Xu, D. Li, *Sensors Actuators, B Chem.*, 230 (2016) 801–809.
6. S. Ferri, K. Kojima, K. Sode, *J. Diabetes Sci. Technol.*, 5 (2011) 1068–1076.
7. S.K. Vashist, D. Zheng, K. Al-Rubeaan, J.H.T. Luong, F.S. Sheu, *Anal. Chim. Acta*, 703 (2011) 124–136.
8. E. Tremey, E. Suraniti, O. Courjean, S. Gounel, C. Stines-Chaumeil, F. Louerat, N. Mano, *Chem. Commun.*, 50 (2014) 5912–5914.
9. E. Tremey, C. Stines-Chaumeil, S. Gounel, N. Mano, *ChemElectroChem*, 4 (2017) 2520–2526.

10. N. Loew, W. Tsugawa, D. Nagae, K. Kojima, K. Sode, *Sensors (Switzerland)*, 17 (2017).
11. S. Cosnier, *Anal. Bioanal. Chem.*, 377 (2003) 507–520.
12. F. Palmisano, P.G. Zambonin, D. Centonze, *Fresenius. J. Anal. Chem.*, 366 (2000) 586–601.
13. K. Sode, N. Loew, Y. Ohnishi, H. Tsuruta, K. Mori, K. Kojima, W. Tsugawa, J.T. LaBelle, D.C. Klonoff, *Biosens. Bioelectron.*, 87 (2017) 305–311.
14. L.C. Jiang, W. De Zhang, *Biosens. Bioelectron.*, 25 (2010) 1402–1407.
15. X. Zhu, Y. Ju, J. Chen, D. Liu, H. Liu, *ACS Sensors*, 3 (2018) 1135–1141.
16. N. Arjona, G. Trejo, J. Ledesma-García, L.G. Arriaga, M. Guerra-Balcázar, *RSC Adv.*, 6 (2016) 15630–15638.
17. S. Yang, G. Li, G. Wang, J. Zhao, X. Gao, L. Qu, *Sensors Actuators, B Chem.*, 221 (2015) 172–178.
18. J. Li, L. Liu, P. Wang, Y. Yang, J. Zheng, *Sensors Actuators, B Chem.*, 198 (2014) 219–224.
19. G. Wang, Z. Jin, M. Zhang, Z.S. Wang, *Part. Part. Syst. Charact.*, 33 (2016) 771–778.
20. K. Shim, W.C. Lee, M.S. Park, M. Shahabuddin, Y. Yamauchi, M.S.A. Hossain, Y.B. Shim, J.H. Kim, *Sensors Actuators, B Chem.*, 278 (2019) 88–96.
21. G. Xiao, J. He, X. Chen, Y. Qiao, F. Wang, Q. Xia, L. Yu, Z. Lu, *Cellulose*, 0123456789 (2019).
22. N. Yusoff, P. Rameshkumar, M.S. Mehmood, A. Pandikumar, H.W. Lee, N.M. Huang, *Biosens. Bioelectron.*, 87 (2017) 1020–1028.
23. U.P. Azad, V. Ganesan, *Electrochim. Acta*, 56 (2011) 5766–5770.
24. S.L. Zhong, J. Zhuang, D.P. Yang, D. Tang, *Biosens. Bioelectron.*, 96 (2017) 26–32.
25. S. Felix, C. Santhosh, A. Nirmala Grace, *ECS Trans.*, 77 (2017) 1847–1857.
26. Z. Sonner, E. Wilder, J. Heikenfeld, G. Kasting, F. Beyette, D. Swaile, F. Sherman, J. Joyce, J. Hagen, N. Kelley-Loughnane, R. Naik, *Biomicrofluidics*, 9 (2015).
27. Y. Zhao, Y. Li, Z. He, Z. Yan, *RSC Adv.*, 3 (2013) 2178–2181.
28. C. Dong, H. Zhong, T. Kou, J. Frenzel, G. Eggeler, Z. Zhang, *ACS Appl. Mater. Interfaces*, 7 (2015) 20215–20223.
29. S. Soyoon, A. Ramadoss, B. Saravanakumar, S.J. Kim, *J. Electroanal. Chem.*, 717–718 (2014) 90–95.
30. H. Huo, C. Guo, G. Li, X. Han, C. Xu, *RSC Adv.*, 4 (2014) 20459–20465.
31. Y. Zhao, X. Bo, L. Guo, *Electrochim. Acta*, 176 (2015) 1272–1279.
32. J. Zhang, J. Ma, S. Zhang, W. Wang, Z. Chen, *Sensors Actuators, B Chem.*, 211 (2015) 385–391.
33. D.L. Zhou, J.J. Feng, L.Y. Cai, Q.X. Fang, J.R. Chen, A.J. Wang, *Electrochim. Acta*, 115 (2014) 103–108.
34. Z. Gao, J. Liu, J. Chang, D. Wu, J. He, K. Wang, F. Xu, K. Jiang, *CrystEngComm*, 14 (2012) 6639–6646.
35. C. Wei, Y. Liu, X. Li, J. Zhao, Z. Ren, H. Pang, *ChemElectroChem*, 1 (2014) 799–807.
36. Y. Liu, Y. Liu, H. Shi, M. Wang, S.H.S. Cheng, H. Bian, M. Kamruzzaman, L. Cao, C.Y. Chung, Z. Lu, *J. Alloys Compd.*, 688 (2016) 380–387.
37. J.M. Marioli, T. Kuwana, *Electrochim. Acta*, 37 (1992) 1187–1197.
38. W. Zheng, Y. Li, L. Hu, L.Y.S. Lee, *Sensors Actuators, B Chem.*, 282 (2019) 187–196.
39. L. Han, S. Zhang, L. Han, D.P. Yang, C. Hou, A. Liu, *Electrochim. Acta*, 138 (2014) 109–114.
40. C. He, J. Wang, N. Gao, H. He, K. Zou, M. Ma, Y. Zhou, Z. Cai, G. Chang, Y. He, *Microchim. Acta*, 186 (2019).
41. D. Xu, C. Zhu, X. Meng, Z. Chen, Y. Li, D. Zhang, S. Zhu, *Sensors Actuators, B Chem.*, 265 (2018) 435–442.